

Orbital symmetries of charge density wave order in $\text{YBa}_2\text{Cu}_3\text{O}_{6+x}$

Christopher McMahon,¹ A. J. Achkar,¹ E. H. da Silva Neto,^{2,3,4,5} I. Djianto,¹
 J. Menard,¹ F. He,⁶ R. Sutarto,⁶ R. Comin,⁷ Ruixing Liang,^{8,3} D. A.
 Bonn,^{2,8,3} W. N. Hardy,^{8,3} A. Damascelli,^{2,8,3} and D. G. Hawthorn^{1,3,*}

¹*Department of Physics and Astronomy,*

University of Waterloo, Waterloo, N2L 3G1, Canada

²*Quantum Matter Institute, University of British Columbia,*

Vancouver, British Columbia V6T 1Z4, Canada

³*CIFAR, Toronto, Ontario M5G 1Z8, Canada*

⁴*Max Planck Institute for Solid State Research,*

Heisenbergstrasse 1, D-70569 Stuttgart, Germany

⁵*Department of Physics, University of California, Davis, California, 95616, USA*

⁶*Canadian Light Source, Saskatoon, Saskatchewan, S7N 2V3, Canada*

⁷*Department of Physics, Massachusetts Institute of Technology, Cambridge, MA, USA*

⁸*Department of Physics & Astronomy,*

University of British Columbia, Vancouver, V6T 1Z1, Canada

* Correspondence and requests for materials should be addressed to D.G.H. (dhawthor@uwaterloo.ca)

Charge density wave (CDW) order has been shown to compete and co-exist with superconductivity in underdoped cuprate superconductors.[1–11] Theoretical proposals for the CDW order include an unconventional d -symmetry form factor CDW[12–21] — a quadrupolar modulation of the charge on oxygen sites surrounding each Cu site — evidence for which has emerged from STM measurements in $\text{Bi}_2\text{Sr}_2\text{CaCu}_2\text{O}_{8+\delta}$ and $\text{Ca}_{2-x}\text{Na}_x\text{CuO}_2\text{Cl}_2$ [22] and resonant soft x-ray scattering (RSXS) measurements of $\text{YBa}_2\text{Cu}_3\text{O}_{6+x}$ (YBCO).[23] Here, we revisit resonant x-ray scattering measurements of the CDW symmetry in YBCO, utilizing a variation in the measurement geometry to provide enhanced sensitivity to the CDW orbital symmetry. We show the $(0\ 0.31\ L)$ CDW peak measured at the Cu L edge is dominated by a simple s form factor rather than a dominant d form factor CDW as was reported previously. In addition, by measuring the CDW orbital symmetry at both $(0.31\ 0\ L)$ and $(0\ 0.31\ L)$, we identify a pronounced difference in the orbital symmetry of the CDW order propagating along the a and b axes, with the CDW propagating along the a -axis exhibiting some form of orbital order in addition to charge order. Model calculations indicate that candidates for the unusual orbital symmetry of the a -axis CDW have large in-plane orbital asymmetry or modulate the orbital orientation.

While the presence of CDW order in the cuprates appears to be ubiquitous, open questions remain about the microscopic character of the CDW order, and whether it is also generic. In particular theoretical studies[12–21] have predicted the CDW charge modulation to have a d form factor in contrast to a more conventional s (s') form factor. Whereas a s (s') CDW involves a simple sinusoidal modulation of the charge density on the Cu (O) sites, a d form factor CDW involves modulations on the bonds between Cu atoms, namely the O sites, that are out-of-phase for bonds oriented along x and y , giving a form-factor with $d_{x^2-y^2}$ symmetry (see fig. 1a). Such a d form factor CDW has been observed in $\text{Bi}_2\text{Sr}_2\text{CaCu}_2\text{O}_{8+\delta}$ and $\text{Ca}_{2-x}\text{Na}_x\text{CuO}_2\text{Cl}_2$ using scanning tunnelling microscopy.[22] Further evidence of a dominant d form factor CDW order was provided non-resonant hard x-ray scattering in YBCO[24] and by resonant soft x-ray scattering (RSXS) measurements at the Cu L edge of the $(0\ 0.31\ 1.48)$ CDW Bragg peak in YBCO.[23] However, the ability of the RSXS measurements to distinguish between dominant d and dominant s or s' factor factor CDW orders was close to the experimental accuracy, providing some ambiguity to the conclusion of a dominant d

form factor CDW order in YBCO. In contrast to these observations, RSXS measurements at the Cu L and O K edges in the spin-charge stripe ordered cuprate $\text{La}_{1.875}\text{Ba}_{0.125}\text{CuO}_4$ (LBCO) find the CDW order to have predominantly s/s' form factor,[25] indicating that the symmetry of the CDW form factor may not be generic to the different cuprate materials. Moreover, Achkar et al.[25] also showed that the orbital symmetry of CDW order is not generic even within YBCO, differing for CDW order propagating along the a and b axes.

In this letter, we present additional RSXS measurements of the orbital symmetry of CDW in YBCO. We follow an experimental approach similar to refs. 23 and 25, but utilize an experimental geometry that provides greater contrast to the d vs. s' or s form factor. Contrary to Comin et al.,[23] we find no clear evidence for a d form factor CDW in YBCO. Rather, measurements of the $(0\ 0.31\ L)$ peak measured at the Cu L appear to be dominated by an s form factor component of the CDW order, similar to LBCO.[25] However, the symmetry of the $(0.31\ 0\ L)$ CDW peak differs from that of the $(0\ 0.31\ L)$ peak and implies a form of orbital order accompanying the charge order propagating along the a axis, adding a new element to other observations of a uni-directional character to CDW order in YBCO.[6, 25–28]

The experimental technique involves measuring the resonant x-ray scattering at the Cu L absorption edge ($\hbar\omega = 931.4\text{eV}$) and the CDW wavevector. At this photon energy, the scattering intensity is sensitive to modulations in the Cu $3d$ or core $2p$ states, and has proven to be an effective probe of CDW order in the cuprates. By varying the photon polarization relative the crystallographic axes, resonant x-ray scattering can also provide insight into the orbital symmetry of the density wave order. This can be understood by considering the CDW scattering intensity, I , on resonance in terms of tensor quantities, akin to the index of refraction in an anisotropic media:

$$I(\vec{Q}, \hbar\omega, \vec{\epsilon}, \vec{\epsilon}') \propto \left| \vec{\epsilon}' \cdot \hat{F}(\vec{Q}, \hbar\omega) \cdot \vec{\epsilon} \right|^2, \quad (1)$$

where $\vec{\epsilon}$ and $\vec{\epsilon}'$ are the incident and scattered polarization vectors, respectively, and

$$\hat{F}(\vec{Q}, \hbar\omega) = \sum_j \hat{f}_j(\hbar\omega) e^{i\vec{Q} \cdot \vec{r}_j} = \begin{bmatrix} F_{aa} & F_{ab} & F_{ac} \\ F_{ba} & F_{bb} & F_{bc} \\ F_{ca} & F_{cb} & F_{cc} \end{bmatrix} \quad (2)$$

is a tensorial expression of the x-ray scattering structure factor. \hat{f}_j is the atomic scattering

form factor tensor for an atom at site, j , and the symmetry of \hat{f}_j follows from the local point group symmetry of that site.[29] Accordingly, the symmetry of $\hat{F}(\vec{Q}, \hbar\omega)$ relates to (but is distinct from) the point group symmetry of individual sites and how that symmetry is modulated by the density wave order.

For instance, a simple s or s' form factor charge density wave order, corresponding to a sinusoidal modulation of charge density (and properties proportional to charge density), would have a scattering tensor that has the same symmetry as the average ($\vec{Q} = 0$) electronic structure. For the CuO_2 planes of YBCO, where holes in Cu $d_{x^2-y^2}$ orbitals dominate the electronic structure that is probed at 931.4 eV, this is approximately D_{4h} symmetry and $\hat{F}(\vec{Q}, \hbar\omega)$ would be a diagonal tensor with $F_{aa} \simeq F_{bb} \gg |F_{cc}|$. In contrast, charge density wave order with a dominant d form factor may feature a symmetry with negative F_{aa}/F_{bb} , indicative of a density modulation on x and y oriented “bonds” that are out-of-phase.[23, 25] This could be seen at the Cu L edge due to shifting in the energy of the Cu $2p_x$ and $2p_y$ core states,[14, 23, 25] or more directly in the occupation of the O $2p$ state by probing the CDW peak at the O K edge.[25] Other symmetries to $\hat{F}(\vec{Q}, \hbar\omega)$ may be signatures of a density wave order that involves orbital order or magnetic order.

Experimentally, the symmetry of $\hat{F}(\vec{Q}, \hbar\omega)$ can be determined by measuring the CDW Bragg peak intensity at a fixed \vec{Q}_{CDW} and rotating the sample azimuthally such that the orientation of $\vec{\epsilon}$ and $\vec{\epsilon}'$ vary relative the the crystallographic axes, as shown in Fig. 1.[23, 25] This approach has been utilized in analysis of the (0 0.31 1.48) peak in YBCO [23] to provide evidence that the CDW has a dominant d form factor. However, the measurements in Comin et. al. [23] utilize a probing geometry with $\Omega \simeq 170^\circ$ ($L \simeq 1.5$) where the CDW peak intensity is maximal. These measurements, while statistically favouring a d form factor, did not provide strong contrast between s , d and s' form factor models. Here we revisit this analysis by measuring the azimuthal dependence of the CDW order at $\Omega \simeq 134^\circ$ ($L \simeq 1.3$) in addition to $\Omega \simeq 170^\circ$ ($L = 1.48$). Notably, the measurements with $\Omega \simeq 134^\circ$ ($L \simeq 1.3$) probe the same CDW peak as $\Omega \simeq 170^\circ$ ($L \simeq 1.48$), owing to the fact that the quasi 2D CDW peak in YBCO is very broad in L . However, the variation in measurement geometry affects how $\vec{\epsilon}$ and $\vec{\epsilon}'$ span the crystallographic axes as ϕ is rotated, yielding greater sensitivity to the sign of F_{aa}/F_{bb} , and thus the form factor of the CDW order, for lower Ω . In addition, we also explore the orbital symmetry of the CDW order measured for both the (0.31 0 L) and (0 0.31 L) peaks, representing CDW order propagating along the a and b axes respectively.

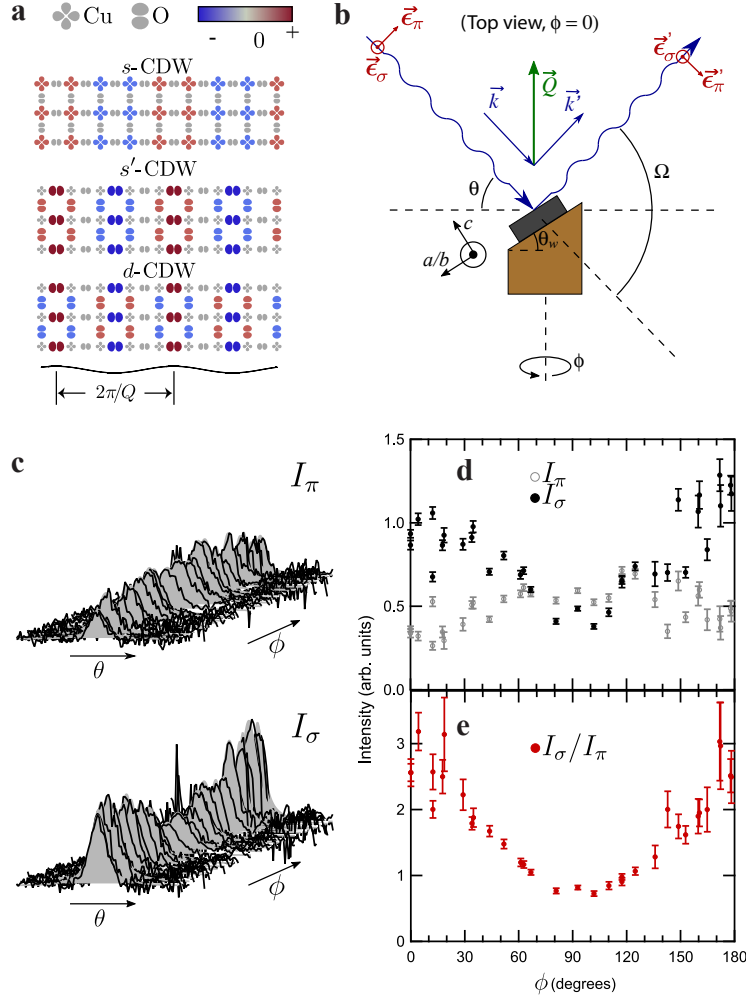


FIG. 1. a) A representation of the CuO₂ planes depicting *s*, *s'* and *d* form factor CDW orders. b) A schematic of the experimental geometry as seen from above showing the orientation when $\phi = 0^\circ$. As ϕ is rotated, the scattering vector \vec{Q} remains unchanged, but the incident ($\vec{\epsilon}$) and scattered ($\vec{\epsilon}'$) photon polarizations vary relative to the crystallographic axes. c) Intensity measurements of the CDW peaks for YBCO-6.75 at (0 0.31 1.32). The peak profiles with fluorescent backgrounds removed as a function of θ and ϕ for π - and σ -polarizations. Lorentzian fits to each peak are shown as grey shading. The amplitudes I_σ and I_π (d) and ratio I_σ/I_π (e) versus azimuthal angle.

The results of the measurements and subsequent fits for the (0 0.31 *L*) and (0.31 0 *L*) peaks using geometries with $L \simeq 1.48$ and $L \simeq 1.33$ are shown in Fig. 2. In addition, data from Comin *et al.*[23] of the (0 0.31 *L*) peak in YBCO-6.75 with $L \simeq 1.48$ are reproduced in Fig. 2(a), and are shown to be in good agreement with our measurements. The first

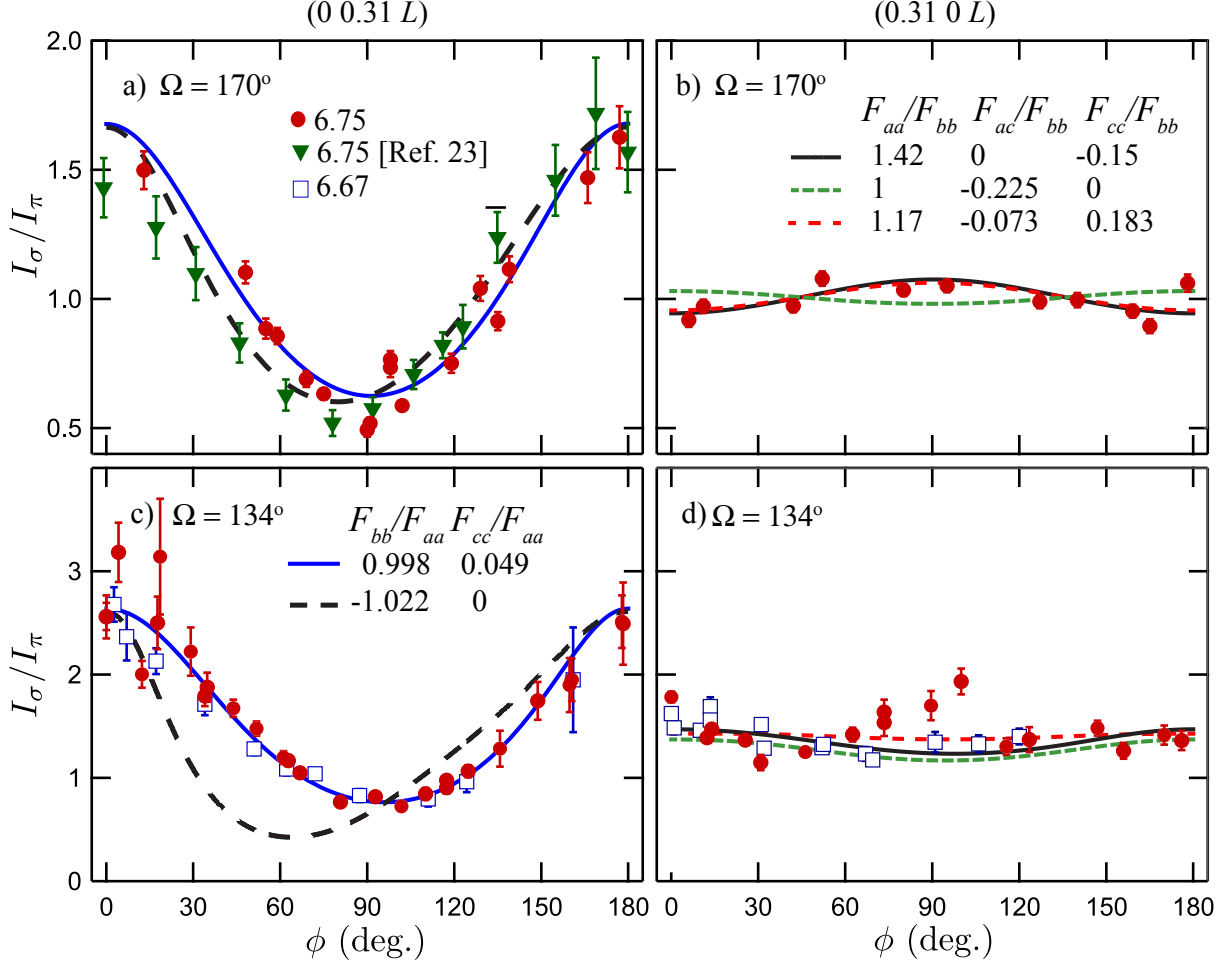


FIG. 2. The ratio of measured scattering intensities with σ and π incident polarization vs. ϕ for the density wave order peaks at $(0 \ 0.31 \ L)$ (a, c) and $(0.31 \ 0 \ L)$ (b, d) for sample with O content 6.67 and 6.75. Data from ref. 23 is reproduced in panel a). The upper row (a, b) shows data taken at $\Omega \simeq 170^\circ$ ($L = 1.48$), while the bottom row (c, d) shows $\Omega \simeq 134^\circ$ ($L = 1.33$). The lines are fits to a model calculations. For the $(0 \ 0.31 \ L)$ peak, a scattering tensor with $F_{aa} \simeq F_{bb} \gg F_{cc}$ agrees well with the data whereas the dominant d form-factor model of ref. 23 (dashed black) does not reproduce the $\Omega = 134^\circ$ data. For the $(0.31 \ 0 \ L)$ peak, a range of parameters corresponding to qualitatively different symmetries provide comparable quality fits.

observation to make about the data in Figure 2 is a striking difference between measurements of the $(0.31 \ 0 \ L)$ and $(0 \ 0.31 \ L)$ peaks, with the $(0 \ 0.31 \ L)$ peaks exhibiting substantially larger dependence on ϕ . We take this as compelling evidence to support the existence of two different orbital symmetries for the CDW order propagating along a and b .

The data in Figure 2 can be fit to determine the components of the scattering and the underlying symmetry of the CDW order. Applying this first to the $(0\ 0.31\ L)$ peak, we note that the fit parameters from Comin et al. used to argue a d form factor CDW, shown as the dashed green line in Figure 2a), agree reasonably well with our measurements for $\Omega = 170^\circ$. However, this model does not agree with our measurements at $\Omega = 134^\circ$ (Fig. 2b), where a minimum in I_σ/I_π at $\phi \simeq 60^\circ$ would be expected instead of the observed minimum at $\phi \simeq 100^\circ$. In contrast, a model with $F_{aa} \simeq F_{bb} \gg |F_{cc}|$ fits well to both $\Omega = 170^\circ$ and 134° measurements (a least squares fit gives $F_{bb}/F_{aa} = 0.998 \pm 0.020$ and $F_{cc}/F_{aa} = 0.049 \pm 0.041$). This symmetry for $\hat{F}(\vec{Q}, \hbar\omega)$ is consistent with the Cu L edge measurements of the CDW order being dominated by an s -form factor component of the CDW order, which would entail a modulation in the orbital occupation (or property proportional to the orbital occupation) of Cu $3d_{x^2-y^2}$ states. In other words, for the $(0\ 0.31\ L)$ peak, the symmetry of the Cu orbitals that are spatially modulated in the CDW is the same as the average symmetry of the in-plane Cu. This symmetry ($F_{aa} \simeq F_{bb} \gg |F_{cc}|$) is similar to that found in Cu L edge measurements of the CDW order in LBCO, where a predominant s' symmetry to the CDW order was also deduced from measurements at the O K edge.[25] It should be noted, however, that since measurements at the Cu L edge are expected to be more sensitive to s components of the CDW order even if a sizeable d component to the form factor is present,[23, 25] the observation that $F_{aa} \simeq F_{bb} \gg F_{cc}$ does not rule out the existence of a d form factor CDW in YBCO, evidence for which has been found from the pattern of oxygen displacements deduced from non-resonant x-ray scattering measurements.[24]

We now turn our attention to fitting the symmetry of $\hat{F}(\vec{Q}, \hbar\omega)$ for the $(0.31\ 0\ L)$ peak. In contrast to the $(0\ 0.31\ L)$ peak, fits of the symmetry of $\hat{F}(\vec{Q}, \hbar\omega)$ show a substantial departure from the average point group symmetry of the CuO_2 planes for the $(0.31\ 0\ L)$. This indicates significant orbital ordering in addition to charge order for the density wave orders propagating along the a axis that is not observed (i.e. is not present or too small to distinguish) along the b axis. Unfortunately, the present measurements are unable to uniquely determine the symmetry of $\hat{F}(\vec{Q}, \hbar\omega)$. Rather, as shown for selected fits in Fig. 2 c) and d), a range of parameters/symmetries with different physical interpretations provide adequate fits to the data (the regions of fit parameters with comparable reduced- χ^2 are shown in supplementary information). This analysis reveals two symmetry distinct scenarios are found to fit well to the data: models having significant in-plane orbital asymmetry $F_{aa} > F_{bb}$

and/or models having off-diagonal $F_{ac} = F_{ca} \neq 0$ elements.

The first scenario, involving a substantial in-plane asymmetry, $F_{aa} > F_{bb}$, may result from a modulation of the in-plane Cu electronic structure that involves Cu $3d$ orbitals beyond simply the $3d_{x^2-y^2}$ states that are known to dominate the low energy electronic structure of the CuO_2 planes. Alternately, $F_{aa} > F_{bb}$, may be indicative of a chain layer contribution to the scattering. However, analysis of the energy dependence of the CDW resonant x-ray scattering did not reveal a contribution to the CDW peak from Cu in the chain layer, which resonates at different photon energies than the Cu in the CuO_2 planes.[5, 30] Moreover, the azimuthal dependence of the $(0.31\ 0\ L)$ peak does not vary as a function of temperature (Fig. 3) or doping (Fig. 2), ruling out contributions from ortho chain ordering to the $(0.31\ 0\ L)$ peak.

The second scenario, the sizeable off-diagonal $F_{ac} = F_{ca}$ terms indicate a density wave order with significant breaking of bc and ab plane mirror symmetries. This could occur if the orientation of the unoccupied Cu d orbitals oscillates about the b -axis such that the bc and ab plane mirror symmetry of an individual Cu site is broken and modulated with period of the CDW. Such a state may be consistent with the previously reported pattern of lattice displacements refined from non-resonant hard x-ray scattering[24] As depicted in Fig. 4, these lattice displacements may result in both a modulation of the orbital occupation and orbital orientation which would be consistent with the presence of finite $F_{ac,ca}$ terms in the scattering tensor. However, since similar patterns of lattice displacements for CDW order along the a and b axes are deduced from non-resonant x-ray scattering,[24] we may have expected to observe off diagonal terms in the $(0\ 0.31\ L)$ as well.

The key question that arises from these results is why the $(0.31\ 0\ L)$ and $(0\ 0.31\ L)$ peaks exhibit different orbital symmetries. In many respects, the density waves orders along a and b appear similar, having comparable correlation lengths, temperature dependencies, energy dependence, intensities at $1/8$ doping and patterns of lattice displacements.[5, 6, 24, 26] However, they also have key differences, such as different doping dependence to their intensities [6, 26] and response to applied magnetic field.[28] A explanation of these differences may lie in identifying the origin of the different orbital symmetries of the density wave orders along a and b .

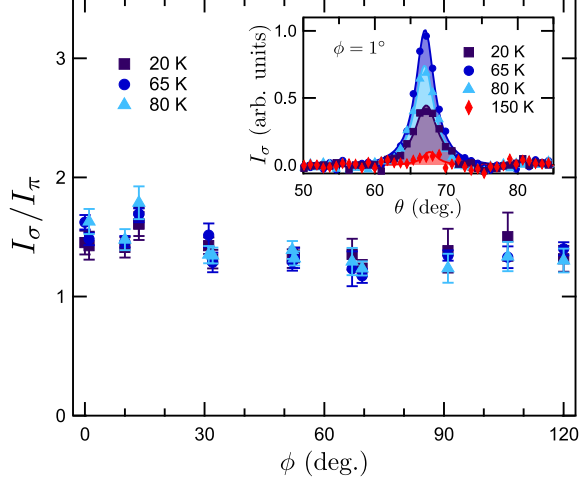


FIG. 3. Measurement of the $(0.31\ 0\ 1.32)$ peak in YBCO-6.67 for a series of temperatures and azimuthal rotations, ϕ . The data overlaps within uncertainty and show no sign of a temperature dependence in the form factor. Inset: Scans of the intensity of the $(0.31\ 0\ 1.33)$ peak with σ polarization at $\phi = 1^\circ$ at various temperatures.

METHODS

Measurements were performed at the REIXS beamline of the Canadian Light Source synchrotron.[31] Samples were mounted on a copper plug angled at $\theta_w = 32.5^\circ$ and 35.5° to achieve a $L = 1.48$ and $L = 1.33$, respectively, as depicted in fig. 1 a). The photon energy was set to 931.3 eV, the peak of the Cu L_3 absorption edge where the CDW ordering peak is maximal.[3, 5] The incident photon polarization was set to either σ and π . However, the scattered photon polarization or energy is not resolved. H and K scans at various ϕ values were performed by rocking θ at fixed Ω such that the peak is centered at a fixed Q_{CDW} that does not vary with ϕ . $\phi = 0$ is defined in Fig. 1 and relates to α from Ref. 23 by $\alpha = 180^\circ - \phi$.

Two single-crystal samples of $\text{YBa}_2\text{Cu}_3\text{O}_{6+x}$ with oxygen stoichiometry of $x = 0.75$ and 0.67 , respectively, were measured utilizing the same samples from previous experiments in Refs. 25, 32. The CDW peak amplitudes were determined by first subtracting a fluorescent background using a fifth-order polynomial and then fitting the CDW peaks to a Lorentzian function, similar to ref. 25. Variations in the details of the fitting procedure were explored and showed little effect on the ϕ dependence of I_σ/I_π . Analysis of the symmetry of $\hat{F}(\vec{Q}, \hbar\omega)$

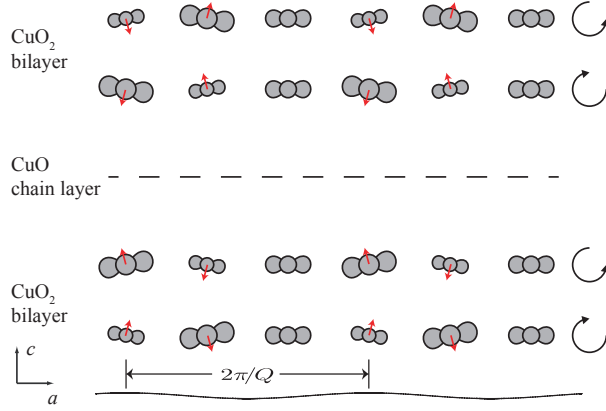


FIG. 4. A simplified pattern of modulated charge (depicted by the size of the Cu 3d orbitals) and orbital symmetry that would give rise to off-diagonal, F_{ac} , elements in $\hat{F}(\vec{Q}, \hbar\omega)$. The pattern of lattice displacements of the Cu atoms deduced from non-resonant x-ray diffraction are shown as red arrows.[24] These displacements trace out ellipses in the ac plane as position advances along the a axis. These displacements (as well as the displacements of the neighbouring O, Y and Ba atoms) break and modulate the local bc and ab plane mirror symmetries. This modulation can lead to an alternation in the orbital occupation (charge) of the Cu (roughly associated with the proximity of the in-plane Cu to the chain layer) and the direction of atomic displacements can lead to an alternation in the orientation of the unoccupied orbitals. A more realistic model must incorporate the impact of O displacements on Cu 3d orbital occupation.

included the impact of the polarization dependence of the absorption coefficient on the scattering intensity, as detailed in Ref. 25. Figure 1 a) and b) show the $(0\ 0.31\ L)$ peak intensities vs. ϕ of the YBCO-6.75 sample on the 35.5° plug with backgrounds removed.

Acknowledgments: The authors acknowledge insightful discussions with S. Hayden, J. van Wezel and G. A. Sawatzky. This work was supported by the Canada Foundation for Innovation (CFI), CIFAR and the Natural Sciences and Engineering Research Council of Canada (NSERC). Research described in this paper was performed at the Canadian Light Source, which is funded by the CFI, the NSERC, the National Research Council Canada, the Canadian Institutes of Health Research, the Government of Saskatchewan, Western Economic Diversification Canada, and the University of Saskatchewan. The work at UBC was supported by the Max Planck-UBC-UTokyo Centre for Quantum Materials and the Canada First Research Excellence Fund, Quantum Materials and Future Technologies Program.

This research was undertaken thanks in part to funding from the Killam, Alfred P. Sloan, and NSERC's Steacie Memorial Fellowships (A.D.), the Alexander von Humboldt Fellowship (A.D.), the Canada Research Chairs Program (A.D.), and CIFAR Quantum Materials Program.

-
- [1] Tranquada, J. M. *et al.* Evidence for stripe correlations of spins and holes in copper oxide superconductors. *Nature* **375**, 561–563 (1995).
 - [2] Wu, T. *et al.* Magnetic-field-induced charge-stripe order in the high-temperature superconductor $\text{YBa}_2\text{Cu}_3\text{O}_y$. *Nature* **477**, 191–194 (2011).
 - [3] Ghiringhelli, G. *et al.* Long-range incommensurate charge fluctuations in $(\text{Y,Nd})\text{Ba}_2\text{Cu}_3\text{O}_{6+x}$. *Science* **337**, 821–5 (2012).
 - [4] Chang, J. *et al.* Direct observation of competition between superconductivity and charge density wave order in $\text{YBa}_2\text{Cu}_3\text{O}_y$. *Nature Physics* **8**, 871–876 (2012).
 - [5] Achkar, A. J. *et al.* Distinct Charge Orders in the Planes and Chains of Ortho-III-Ordered $\text{YBa}_2\text{Cu}_3\text{O}_{6+x}$ Superconductors Identified by Resonant Elastic X-ray Scattering. *Physical Review Letters* **109**, 167001 (2012).
 - [6] Blackburn, E. *et al.* X-ray diffraction observations of a charge-density-wave order in superconducting ortho-II $\text{YBa}_2\text{Cu}_3\text{O}_{6.54}$ single crystals in zero magnetic field. *Physical Review Letters* **110**, 137004 (2013).
 - [7] Comin, R. *et al.* Charge Order Driven by Fermi-Arc Instability in $\text{Bi}_2\text{Sr}_{2-x}\text{La}_x\text{CuO}_{6+d}$. *Science* **343**, 390–392 (2014).
 - [8] da Silva Neto, E. H. *et al.* Ubiquitous Interplay Between Charge Ordering and High-Temperature Superconductivity in Cuprates. *Science* **343**, 393–396 (2014).
 - [9] da Silva Neto, E. H. *et al.* Charge ordering in the electron-doped superconductor $\text{Nd}_{2-x}\text{Ce}_x\text{CuO}_4$. *Science* **347**, 282–285 (2015).
 - [10] Tabis, W. *et al.* Charge order and its connection with Fermi-liquid charge transport in a pristine high- T_c cuprate. *Nature Communications* **5**, 5875–5875 (2014).
 - [11] Kohsaka, Y. *et al.* An Intrinsic Bond-Centered Electronic Glass with Unidirectional Domains in Underdoped Cuprates. *Science* **315**, 1380–1385 (2007).

- [12] Metlitski, M. A. & Sachdev, S. Quantum phase transitions of metals in two spatial dimensions. II. Spin density wave order. *Physical Review B* **82**, 075128 (2010).
- [13] Sachdev, S. & La Placa, R. Bond order in two-dimensional metals with antiferromagnetic exchange interactions. *Physical Review Letters* **111**, 027202 (2013).
- [14] Efetov, K. B., Meier, H. & Pépin, C. Pseudogap state near a quantum critical point. *Nature Physics* **9**, 442–446 (2013).
- [15] Seo, K., Chen, H. D. & Hu, J. D-wave checkerboard order in cuprates. *Physical Review B* **76**, 020511 (2007).
- [16] Vojta, M. & Rösch, O. Superconducting d -wave stripes in cuprates: Valence bond order coexisting with nodal quasiparticles. *Physical Review B* **77**, 094504 (2008).
- [17] Atkinson, W. A., Kampf, A. P. & Bulut, S. Charge order in the pseudogap phase of cuprate superconductors. *New Journal of Physics* **17**, 13025 (2015).
- [18] Lawler, M. J. *et al.* Intra-unit-cell electronic nematicity of the high- T_c copper-oxide pseudogap states. *Nature* **466**, 347–351 (2010). 1007.3216.
- [19] Li, J.-X., Wu, C.-Q. & Lee, D.-H. Checkerboard charge density wave and pseudogap of high- T_c cuprate. *Physical Review B* **74**, 184515 (2006).
- [20] Allais, A., Bauer, J. & Sachdev, S. Density wave instabilities in a correlated two-dimensional metal. *Physical Review B* **90**, 155114 (2014).
- [21] Chowdhury, D. & Sachdev, S. Density-wave instabilities of fractionalized Fermi liquids. *Physical Review B* **90**, 245136 (2014).
- [22] Fujita, K. *et al.* Direct phase-sensitive identification of a d -form factor density wave in underdoped cuprates. *Proceedings of the National Academy of Sciences* **111**, E3026–E3032 (2014).
- [23] Comin, R. *et al.* Symmetry of charge order in cuprates. *Nature Materials* **14**, 796–800 (2015).
- [24] Forgan, E. M. *et al.* The microscopic structure of charge density waves in underdoped $\text{YBa}_2\text{Cu}_3\text{O}_{6.54}$ revealed by X-ray diffraction. *Nature Communications* **6**, 10064 (2015).
- [25] Achkar, A. J. *et al.* Orbital symmetry of charge-density-wave order in $\text{La}_{1.875}\text{Ba}_{0.125}\text{CuO}_4$ and $\text{YBa}_2\text{Cu}_3\text{O}_{6.67}$. *Nature Materials* **15**, 616–620 (2016).
- [26] Blanco-Canosa, S. *et al.* Momentum-dependent charge correlations in $\text{YBa}_2\text{Cu}_3\text{O}_{6+\delta}$ superconductors probed by resonant x-ray scattering: Evidence for three competing phases. *Physical Review Letters* **110**, 187001 (2013).
- [27] Comin, R. *et al.* Broken translational and rotational symmetry via charge stripe order in

- underdoped $\text{YBa}_2\text{Cu}_3\text{O}_{6+y}$. *Science* **347**, 1335–1339 (2015).
- [28] Chang, J. *et al.* Magnetic field controlled charge density wave coupling in underdoped $\text{YBa}_2\text{Cu}_3\text{O}_{6+x}$. *Nature Communications* **7**, 11494 (2016).
- [29] Haverkort, M., Hollmann, N., Krug, I. & Tanaka, A. Symmetry analysis of magneto-optical effects: The case of x-ray diffraction and x-ray absorption at the transition metal $L_{2,3}$ edge. *Physical Review B* **82**, 094403 (2010).
- [30] Hawthorn, D. G. *et al.* Resonant elastic soft x-ray scattering in oxygen-ordered $\text{YBa}_2\text{Cu}_3\text{O}_{6+\delta}$. *Phys. Rev. B* **84**, 075125 (2011).
- [31] Hawthorn, D. G. *et al.* An in-vacuum diffractometer for resonant elastic soft x-ray scattering. *Review of Scientific Instruments* **82**, 073104 (2011).
- [32] Achkar, A. J. *et al.* Impact of quenched oxygen disorder on charge density wave order in $\text{YBa}_2\text{Cu}_3\text{O}_{6+x}$. *Physical Review Letters* **113**, 10700 (2014).

Supplementary information for: Orbital symmetries of charge density wave order in $\text{YBa}_2\text{Cu}_3\text{O}_{6+x}$

In this Supplementary Information, we provide additional details regarding i) extracting the ratio of scattering intensity for σ and π incident photon polarization from the experimental data and ii) assess the range of fit parameters that provide good agreement with the measurements by examining the reduced- χ^2 of model calculations.

Experimental data.

In fig. S1 we provide an example of the experimental data that was used to determine the ϕ dependences of I_σ and I_π shown in the main text. The peak intensities are determined by scanning θ through the CDW peak position. As shown in fig. S1 A and B, at 220 K, above the CDW ordering temperature, a smooth fluorescent background is observed. At 73 K a clear CDW peak is observed in addition to the fluorescent. Measurements both above and below the CDW ordering temperature were not performed at for all samples and peaks. As such, in order to subtract the fluorescent background and determine the peak intensity, we fit a 5th order polynomial to the background (fig. S1 C and D), which is subtracted to reveal the CDW scattering intensity (fig. S1 E and F). The resulting CDW peaks are fit to a Lorentzian line shape to determine the peak intensity vs. ϕ for σ and π incident photon polarization and determine their ratio I_σ/I_π , as shown in figure 1 and 2 of the main text.

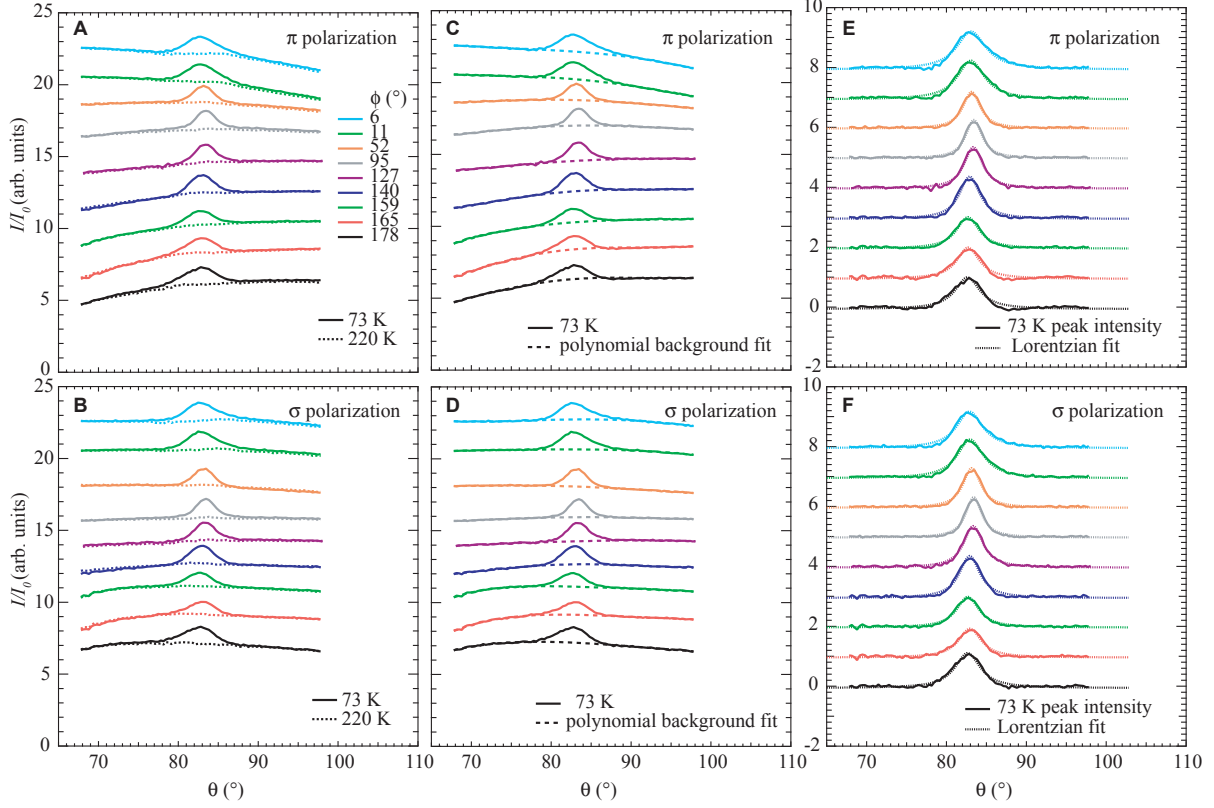


Figure S1: θ scans at various ϕ values through the CDW peak in the $\text{YBa}_2\text{Cu}_3\text{O}_{6.75}$ sample at (0.31 0 1.48) for A) π and B) σ incident photon polarization. For clarity, data at different ϕ values are offset in the y-axis increments of 2 (Measurements at $\phi = 178^\circ$ are not offset. C) and D) fits to the fluorescent background of the data at 73 K using a 5th order polynomial. E) and F) The peak intensity for various ϕ values after subtraction of a polynomial background along with Lorentzian fits to the peaks.

Assessment of the quality of fits and range of parameters that agree with the measurements.

For the (0 0.31 0 L) peak, the measured ratio I_σ/I_π was fit to a model with;

$$\hat{F}(\vec{Q}, \hbar\omega) \sim \begin{bmatrix} F_{aa} & 0 & 0 \\ 0 & F_{bb} & 0 \\ 0 & 0 & F_{cc} \end{bmatrix} \quad (\text{S1})$$

The best fit to the data was achieved with $F_{bb}/F_{aa} = 0.998 \pm 0.020$ and $F_{cc}/F_{aa} = 0.049 \pm 0.041$. The standard deviation, however, does not adequately represent the uncertainty

in the parameters. This is because F_{bb}/F_{aa} and F_{cc}/F_{aa} are not completely independent fitting parameters. Rather, variation in one parameter can be offset with variation in the other in order to improve the fit. A better assessment of the range of parameters that provide good agreement with the data can be achieved by examining the dependence on fit parameters of the reduced χ^2 statistic, as shown in Figure S2 A). Good fits to the data are found in an elliptical range of parameters around the best fit value, where $F_{aa} \simeq F_{bb} \ll F_{cc}$ with a level of agreement comparable to the scatter in the data are roughly found for range of parameters inside the $\chi_0^2 = 5$ contour. A comparison between the measurement and model calculations with selected parameters (shown by the solid circles in fig. S2 A) that have different values of χ_0^2 is shown in Fig. S2 B and C.

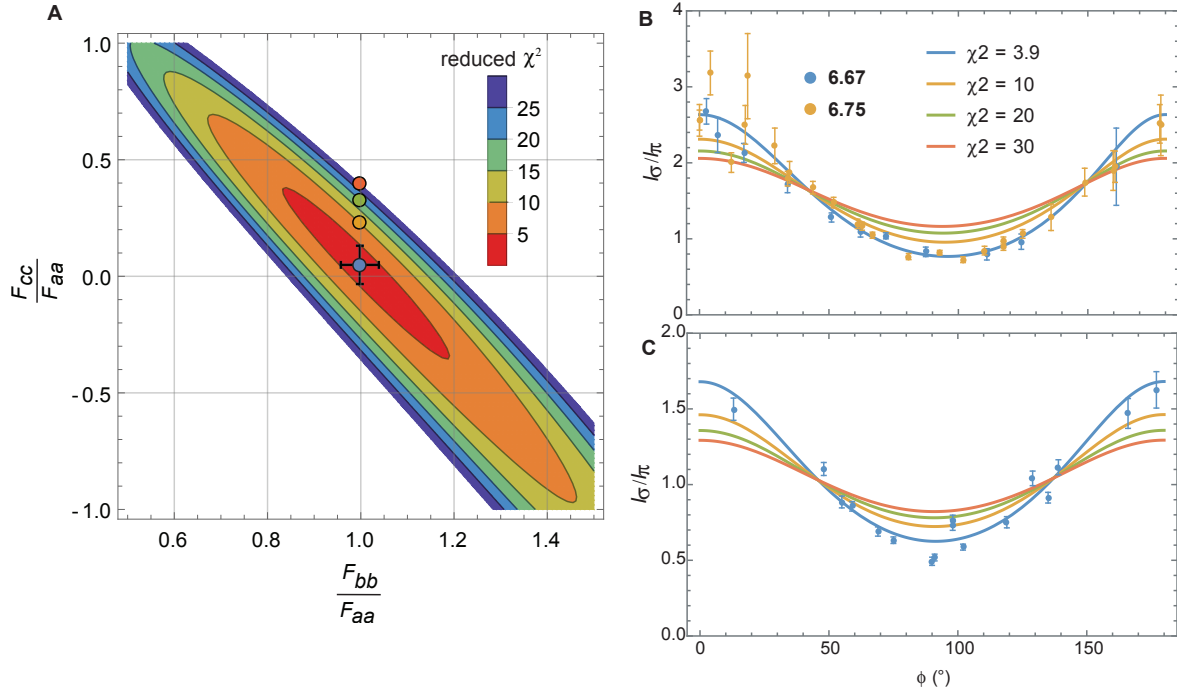


Figure S2: Assessment of the fit quality for the (0 0.31 L) peak. **A** A map of the reduced χ^2 from fits to data at both (0.31 0 1.48) and (0.31 0 1.32) vs. F_{cc}/F_{aa} , and F_{bb}/F_{aa} . The blue circle represents the best fit value. **B** and **C** Examples of I_σ/I_π vs. ϕ calculated for different reduced χ^2 values. The curves in **B** and **C** were calculated using parameters given by the point in **A** of the same colour as the curve.

For the (0.31 0 0 L) peak, the measured ratio I_σ/I_π was fit to a more a general model with off-diagonal terms $F_{ac} = F_{ca}$, indicative of broken bc and ab plane mirror symmetries:

$$\hat{F}(\vec{Q}, \hbar\omega) \sim \begin{bmatrix} F_{aa} & 0 & F_{ac} \\ 0 & F_{bb} & 0 \\ F_{ac} & 0 & F_{cc} \end{bmatrix} \quad (\text{S2})$$

The best fit to the data on the 6.75 sample gave $F_{ac}/F_{bb} = -0.073$, $F_{cc}/F_{bb} = 0.183$, and $F_{aa}/F_{bb} = 1.172$. In figure S3 we present the variation of reduced χ^2 statistic with model parameters. As shown, a range of model parameters provide good agreement with the data with fits with reduced $\chi^2 < 10$ all provide similar quality, comparable to the scattering in the data. This region with $\chi^2 < 10$ includes models with $F_{ac} = 0$ and F_{aa}/F_{bb} significantly greater than 1, models that retain ab and bc plane mirror symmetries but has significant in-plane asymmetry. However, it also includes a model with $F_{aa} \simeq F_{bb}$ and $F_{ac} = -0.22$, a model that breaks ab and bc plane mirror symmetries but retains approximate in-plane asymmetry of the diagonal elements, similar to the (0 0.31 L) peak.

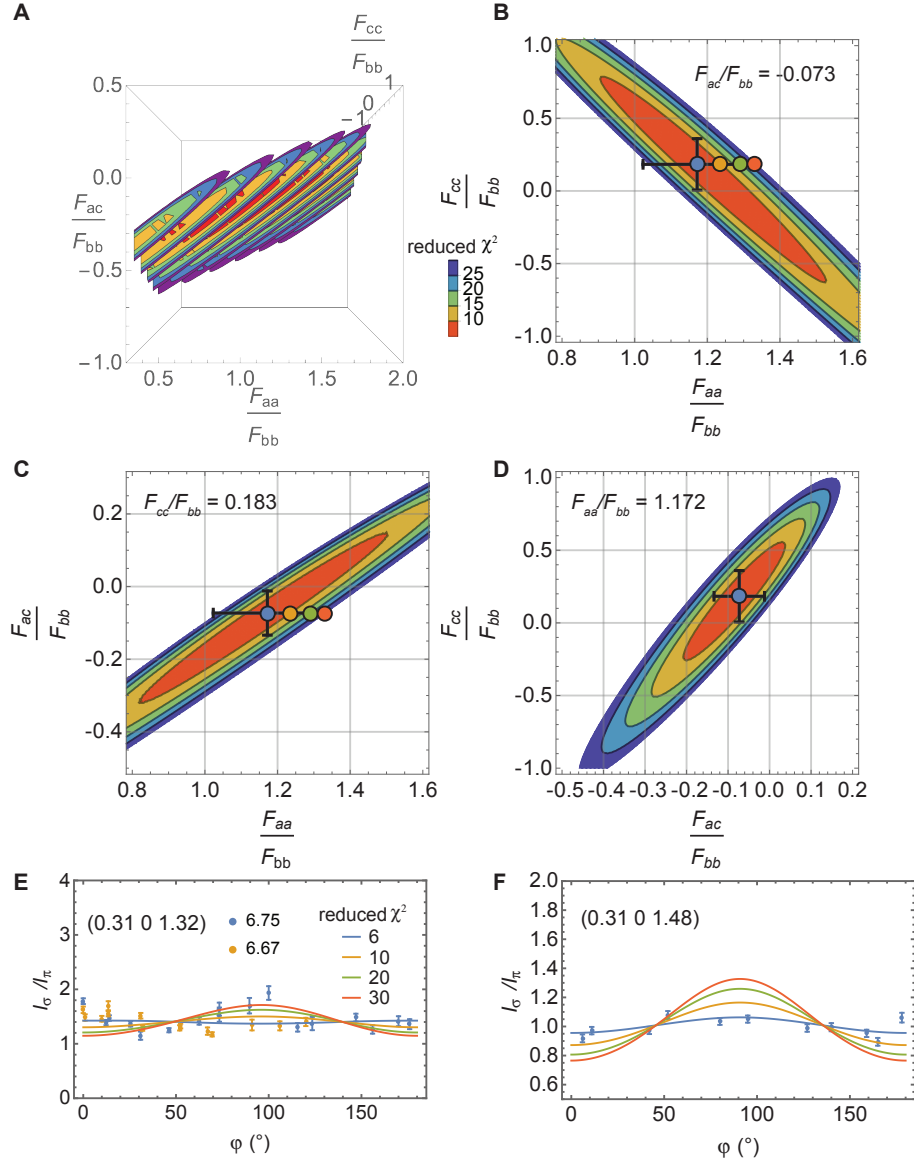


Figure S3: Assessment of the fit quality for the (0.31 0 L) peak. **A** A map of the reduced χ^2 from fits to the 6.75 data at both (0.31 0 1.48) and (0.31 0 1.32) vs. F_{ac}/F_{bb} , F_{cc}/F_{bb} , and F_{aa}/F_{bb} . Contours of constant χ^2 are shown as slices through the 3D parameter space. **B**, **C** and **D** 2D slices of reduced- χ^2 through the best fit value $F_{ac}/F_{bb} = -0.073$, $F_{cc}/F_{bb} = 0.183$, and $F_{aa}/F_{bb} = 1.172$. The blue circle represents the best fit value and the error bars denote the 95% confidence interval of the fit. **E** and **F** Examples of I_σ/I_π vs. ϕ calculated for different reduced χ^2 values. The curves in **E** and **F** were calculated using parameters given by the point in **C** and **D** of the same colour as the curve.